American College of Neuropsychopharmacology

www.nature.com/npp

ARTICLE

Check for updates

Extinction training suppresses activity of fear memory ensembles across the hippocampus and alters transcriptomes of fear-encoding cells

Alfredo Zuniga[1,2,6,7], Jiawei Han[3,4,7], Isaac Miller-Crews[3], Laura A. Agee[1,2], Hans A. Hofmann[3,4,5]✉ and Michael R. Drew[1,2,5]✉

Contextual fear conditioning has been shown to activate a set of "fear ensemble" cells in the hippocampal dentate gyrus (DG) whose reactivation is necessary and sufficient for expression of contextual fear. We previously demonstrated that extinction learning suppresses reactivation of these fear ensemble cells and activates a competing set of DG cells—the "extinction ensemble." Here, we tested whether extinction was sufficient to suppress reactivation in other regions and used single nucleus RNA sequencing (snRNA-seq) of cells in the dorsal dentate gyrus to examine how extinction affects the transcriptomic activity of fear ensemble and fear recall-activated cells. Our results confirm the suppressive effects of extinction in the dorsal and ventral dentate gyrus and demonstrate that this same effect extends to fear ensemble cells located in the dorsal CA1. Interestingly, the extinction-induced suppression of fear ensemble activity was not detected in ventral CA1. Our snRNA-seq analysis demonstrates that extinction training markedly changes transcription patterns in fear ensemble cells and that cells activated during recall of fear and recall of extinction have distinct transcriptomic profiles. Together, our results indicate that extinction training suppresses a broad portion of the fear ensemble in the hippocampus, and this suppression is accompanied by changes in the transcriptomes of fear ensemble cells and the emergence of a transcriptionally unique extinction ensemble.

Neuropsychopharmacology; https://doi.org/10.1038/s41386-024-01897-0

INTRODUCTION

Although fear-based learning is important for survival, learned fear that is excessive and/or overgeneralized —as is seen in clinical phobias or post-traumatic stress disorder—can be debilitating. The front-line behavioral methods for treating such fear-related disorders are based on extinction. In these treatments, patients are repeatedly exposed to the feared stimuli in a safe context [1]. This will ideally produce fear extinction, a lasting decrease in the behavioral response to the feared stimuli and a critical component of adaptive and context-appropriate behavior [2]. Unfortunately, fear often relapses after extinction. For instance, in spontaneous recovery the fear response returns with the passage of time after the conclusion of extinction training [3]. The existence of spontaneous recovery and other forms of relapse imply that, rather than abolishing or otherwise altering the fear memory, extinction training works by inducing formation of a competing "extinction memory" that inhibits expression of the fear memory.

Research on the neural mechanisms of extinction has identified the hippocampus as a crucial structure in this form of learning. Disruption of hippocampal activity both interferes with extinction learning [4–6] and can alter generalization of the extinction memory to other contexts [7–9]. Studies using immediate early gene (IEG)-based trapping approaches to tag cells active in a specific timeframe demonstrate that the hippocampus generates ensemble representations of both contextual fear and contextual fear extinction [6, 10–13]. Neurons active during contextual fear conditioning (CFC)—the fear ensemble—are reactivated during recall of the memory, and this reactivation is both necessary and sufficient for expression of contextual fear. We recently demonstrated that extinction training suppresses reactivation of the fear ensemble within the hippocampal dentate gyrus (DG) and activates a separate set of cells, the putative extinction ensemble [6]. Whereas artificial stimulation of the fear ensemble increases fear, stimulation of this extinction ensemble reduces it.

In the present study, we investigate the effects of extinction training on IEG activity and gene expression in the hippocampal fear ensemble. We first set out to evaluate the generality of the effects of extinction on the fear ensemble. In Lacagnina et al. [6], extinction was shown to suppress expression of the IEG Arc in DG fear neurons; other regions and activity markers were not evaluated. Here, we asked whether the suppressive effect of extinction was present beyond the DG, whether this effect was present across the dorsoventral axis of the hippocampus, and whether it could be observed with another canonical IEG, c-Fos. A second objective was to characterize the effects of extinction training on the transcriptomes of fear acquisition neurons. Our results demonstrate that

[1]Department of Neuroscience, The University of Texas at Austin, Austin, TX, USA. [2]Center for Learning and Memory, University of Texas at Austin, Austin, TX, USA. [3]Department of Integrative Biology, The University of Texas at Austin, Austin, TX, USA. [4]Interdisciplinary Life Sciences Graduate Programs, The University of Texas at Austin, Austin, TX, USA. [5]Institute for Neuroscience, The University of Texas at Austin, Austin, TX, USA. [6]Present address: Department of Neuroscience, The College of Wooster, 1189 Beall Ave, Wooster, OH 44691, USA. [7]These authors contributed equally: Alfredo Zuniga, Jiawei Han. ✉email: hans@utexas.edu; drew@mail.clm.utexas.edu

Received: 2 January 2024 Revised: 6 May 2024 Accepted: 30 May 2024
Published online: 14 June 2024

extinction training causes a robust suppression of both Arc and c-Fos expression in the hippocampal fear ensemble throughout the dorsal and ventral DG and dorsal CA1. This suppression is accompanied by profound transcriptional changes in the fear ensemble, providing novel insights into the molecular mechanisms through which extinction suppresses learned fear.

MATERIALS AND METHODS

Animals

Adult male and female ArcCreERT2::eYFP mice (12–15 weeks) were used for all experiments. For experiment 1 (Figs. 1–3), 12 mice were used (6 per group). An additional 6 mice were used for experiment 2 (Figs. 4, 5). Mice were generated by breeding pairs gifted by Dr. Christine Denny [11]. Briefly, heterozygous (+/−) ArcCreERT2::(+/+) R26R-STOP-floxed-eYFP mice were crossed with homozygous (−/−) ArcCreERT2::(+/+) R26R-STOP-floxed-eYFP mice. These crosses generated mice that were heterozygous (+/−) for the ArcCreERT2 allele and homozygous (+/+) for the eYFP allele. Mice were housed in groups (4–5 per cage) until 7 d prior to the start of the experiment, at which point they were individually housed in plastic cages with woodchip bedding. Mice were kept on a 12 h light/dark cycle (lights on at 07:00) with *ad libitum* access to food and water. All protocols were reviewed and approved by the University of Texas at Austin Institutional Animal Care and Use Committee.

Neuronal tagging

Recombination was induced with 4-hydroxytamoxifen (4-OHT, Sigma-Aldrich), as previously reported [6, 11]. 4-OHT (10 mg/mL) was dissolved via sonication in a 10% ethanol/90% sunflower seed oil solution. To minimize transportation- and novelty-induced IEG activity, mice were transported to a separate housing room near the conditioning room 24 h prior to fear conditioning and 4-OHT injections. Neuronal tagging was induced by a single intraperitoneal injection of 4-OHT (55 mg/kg) given immediately following the contextual fear conditioning session. Following the 4-OHT injection, mice were placed back in the housing room for 72 h during which they were housed in the dark as previously described [11] and then returned to the vivarium with a 12 h light/dark cycle for the duration of the experiment.

Contextual fear conditioning

All mice were handled once a day for 1–2 min for 3 d prior to the commencement of fear conditioning. Mice were moved individually from their home cage to and from the conditioning room in an opaque container with a clear lid. Transport containers were cleaned between mice with 70% ethanol.

Fear conditioning, extinction, and testing occurred in conditioning chambers (30.5 × 24 × 21 cm, Med Associates) scented with 1% acetic acid in the waste tray located below the floor. The fear conditioning protocol consisted of three 2-s, 0.75 mA scrambled foot shocks delivered via the floor 180, 240, and 300 s after mice were placed in the chambers. Mice were removed from the conditioning chambers and returned to their home cages 30 s after the final foot shock. All behavior was recorded at 30 frames per second using a near-infrared camera. Freezing was scored using VideoFreeze Software (Med Associates).

Extinction and testing

Extinction sessions consisted of a 5-min exposure to the conditioning context without the presentation of a shock. Mice in the *Extinction* group were exposed to extinction training once a day for 10 days. Mice in the *No Extinction* group were left undisturbed in their home cages (in the vivarium) during these sessions. 72 h after the last extinction session, all mice were exposed to a final 5 min CFC test in the conditioning context.

Tissue collection and processing

Mice were euthanized following the conclusion of the final behavioral test, and tissue was collected in one of two ways depending on whether tissue was to be processed for immunohistochemistry or single nuclei RNA sequencing (snRNA-seq). For immunohistochemistry, mice were anesthetized with ketamine/xylazine (150/15 mg/kg) 90 min after the end of behavioral testing and transcardially perfused with 1X PBS followed by 4% paraformaldehyde (PFA) in 1X PBS. Brains were extracted and fixed in 4% PFA, then immersed in 20–30% sucrose for 48 h. Finally, brains were cryosectioned at 35 µm and stored in cryo-protectant at −20 °C. For snRNA-seq, mice were anesthetized with 5% isoflurane and then rapidly decapitated 30 min after the final behavioral test. Brains were extracted and flash-frozen in OCT cryostat embedding medium (Sakura Finetek) and then stored at −80 °C until further processing.

Immunohistochemistry and imaging

Eight to ten sections (per mouse) encompassing the dorsal and ventral hippocampus (Bregma −1.7 to −3.64 mm) were processed for immunohistochemistry as described in Supplementary Methods. For each animal, 3–4 sections per region were imaged, counted, and analyzed. Sections were imaged at 20X magnification across the z-plane (5–7 images per z-stack) on a Zeiss Axio Imager M2 (Zeiss) and counted using Stereo Investigator software (Mbf).

snRNA-seq

Frozen brains were transferred to a cryostat and sectioned at 300 µm directly onto glass slides and kept cold on dry ice. The dorsal DG was micro-dissected using a disposable tissue punch tool (Electron Microscopy Sciences; diameter: 0.75 mm). We adapted the protocol by Martelotto [14] for nuclei isolation directly from flash-frozen tissue for use with 10x Genomics Chromium Single Cell 3′ Reagent Kit (cat. pn-1000075; 10x Genomics, USA). See Supplementary Methods for details on microdissection and isolation of nuclei.

Library construction and sequencing were performed at the Genomic Sequencing and Analysis Facility at The University of Texas at Austin. Briefly, samples were loaded on the Chromium Next GEM Single Cell 3′ reagent kits v3.1 as per manufacturer's instructions, with ~10,000 nuclei per pool as a target. Following the guidance of Davis et al. [15] and Schmid et al. [16], we estimated that we needed to sequence 7,385 cells/pool from ~3 samples to detect two cell populations with as few as ~20 cells/pool with 99% power. The libraries were sequenced on an Illumina HiSeq 2500 platform (Illumina, USA), generating 930 million reads, with 460 million reads per sample on average. All reads had Phred scores above 35 and passed all quality control measures (MultiQC) [17]. All sequence data have been submitted to NCBI (accession number PRJNA1122232).

Bioinformatics and statistics

The data from all behavioral and immunohistochemical experiments were analyzed using the base statistics functions in R alongside statistical functions from the dplyr [18], rstatix [19], and emmeans [20] packages. Specifically, we used t-tests and analysis of variance (ANOVA). Tukey HSD tests were used for post-hoc comparisons. If assumptions of normality were not met, we log-transformed the data. Effect sizes were calculated using the untransformed data and reported as the generalized eta-squared (η_G^2) [21] for the full ANOVAs or Cohen's d for post-hoc pairwise comparisons. For the two pooled snRNA-seq samples, FASTQ files were generated after demultiplexing and subjected to quality control by FAST-QC (Babraham Bioinformatics). Cellranger counts (Cell Ranger 6.1, 10x Genomics) were used to perform alignment, filtering, barcode counting, and UMI counting on the FASTQ files. All reads were mapped to mouse genome, mm10-2020-A. Output files were used to generate Seurat object using Seurat V4.0 [22] in R. Datasets from both samples were pre-processed with the Seurat pipeline with baseline filtering parameters of min.cells = 3 and min.features = 200. The count matrix was filtered to remove empty droplets, doublets and triplets, yielding a total of 8467 nuclei for the No-Extinction sample and 103041 nuclei for the Extinction sample. The data were log-normalized using the NormalizeData function, and highly variable genes were identified using the FindVariableFeatures function. Integrated analysis across the two samples was performed using the Seurat Integration analysis pipeline, generating 24 clusters (FindNeighbors and FindClusters, using first 30 principal components), which were later characterized as 9 putative cell types. Differentially expressed genes (DEGs: $p < 0.05$, $\log_2$ fold-change >0.2) were identified using the R package *limma* Trend [23], and volcano plots were generated using the EnhancedVolcano R package (https://github.com/kevinblighe/EnhancedVolcano). We used the Single Cell Proportion Test (https://github.com/rpolicastro/scProportionTest) with 10,000 permutations to estimate the proportional difference between treatment in cell number across clusters. Functional enrichment analysis was carried out using Metascape [24] to discover enriched Gene Ontology (GO) terms or Kyoto Encyclopedia of Genes and Genomes pathways. Enriched terms were required to include ≥3 candidates, with a $p \leq 0.01$ and an enrichment factor ≥1.5.

RESULTS

Behavior

We compared freezing levels at final recall between mice that had undergone extinction (Ext group) and those that had not (No Ext

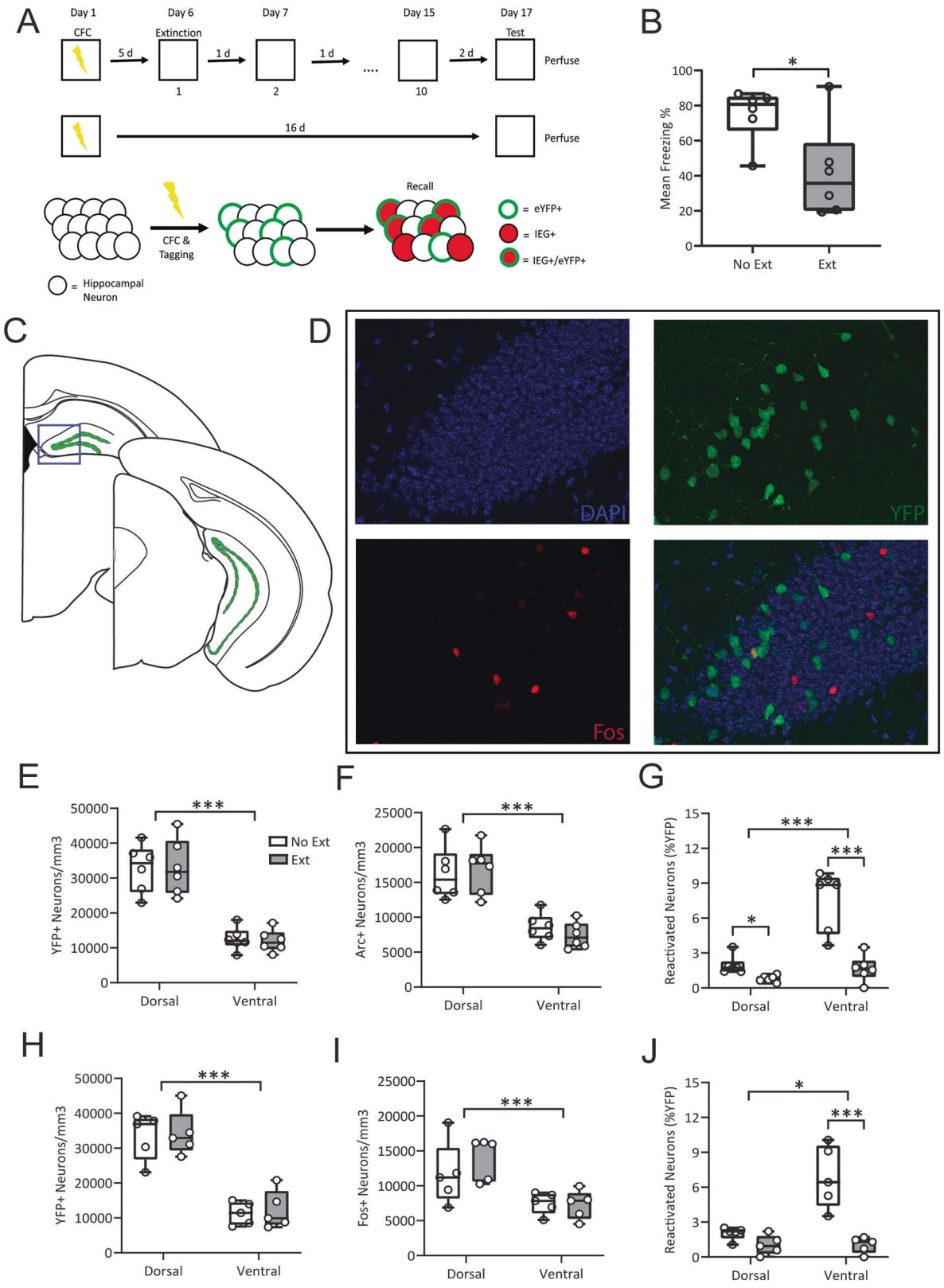

group; Fig. 1A). As expected, a between-subjects t-test showed that mice that underwent extinction training following CFC exhibited significantly less freezing at the final recall test than mice that did not receive extinction training [Fig. 1B; $t(10) = 2.66$, $p = 0.029$].

Immediate-early gene protein expression in fear ensembles

Extinction training suppresses reactivation of fear ensembles in the dorsal and ventral DG. Using this procedure we previously demonstrated that extinction training suppresses reactivation of DG fear acquisition neurons [6]. We sought to replicate this finding

Fig. 1 Extinction training suppresses Arc and Fos in YFP+ fear neurons across the dorsal-ventral axis of DG. A Experimental design. ArcCreERT2::eYFP mice were injected with 4-hydroxytamoxifen immediately following contextual fear conditioning (CFC) to tag CFC-activated neurons. Mice then either underwent fear extinction (*Ext group)* or were left undisturbed (*No Ext group)* before being re-exposed to the CFC context and having their tissue processed for Arc or c-Fos expression. **B** Coronal slices displaying (in green) representative locations from which dorsal (back) and ventral (front) dentate gyrus (DG) cells counts were taken. The blue box identifies where representative images (in **D**) were taken. **C** Mice that received extinction training displayed significantly less context freezing on the final testing day. **D** Representative micrographs of YFP and Fos immunofluorescence in the DG. Tissue processed for Arc expression (**E**–**G**) showed no group differences in YFP+ or Arc+ cells in either the dorsal or ventral DG. Tissue processed for c-Fos expression (**H**–**J**) similarly showed no difference in overall YFP+ or Fos+ cell counts. In contrast, *No Extinction* mice displayed significantly higher levels of Arc+/YFP+ reactivated cells (**G**) and Fos+/YFP+ reactivated cells (**J**) in both the dorsal and ventral DG in comparison to mice in the *Extinction* group. * $p < 0.05$, ** $p < 0.01$, *** $p < 0.001$.

and assess its generality across the dorsoventral axis of the various hippocampal subregions. We first used YFP to identify DG neurons that were active during fear conditioning, Arc protein expression to identify neurons active during the test, and overlap of both markers to identify fear ensemble cells reactivated at final testing (%YFP+ cells expressing Arc; Fig. 1C, D). Expression of these markers was assessed in the dorsal and ventral DG, and expression across groups was compared using two-way mixed ANOVAs. We found no significant differences in expression of YFP or Arc between the Ext and No Ext groups in the dorsal or ventral DG (Fig. 1E, F; all $p > 0.1$). There were, however, significantly more Arc+ [$F(1, 10) = 69.08$, $p < 0.0001$, $\eta_G^2 = 0.724$] and YFP+ [$F(1, 10) = 146.83$, $p < 0.0001$, $\eta_G^2 = 0.794$] cells in the dorsal than the ventral DG. Importantly, we found that reactivation was reduced in the Ext group compared to No Ext mice [$F(1,10) = 23.43$, $p < 0.001$, $\eta_G^2 = 0.557$] and significantly different between region (dorsal vs. ventral DG) [$F(1,10) = 22.877$, $p < 0.001$, $\eta_G^2 = 0.504$] with an interaction between treatment and region [$F(1,10) = 8.499$, $p = 0.015$, $\eta_G^2 = 0.376$] (Fig. 1G). Tukey HSD test comparisons using estimated marginal means determined that the effect of treatment was present in both the dorsal [$t = 2.275$, $p = 0.0354$, $d = 2.29$] and ventral [$t = 5.636$, $p < 0.0001$, $d = 2.5$] DG, with overall fear ensemble reactivation levels being higher in the ventral DG.

Extinction training suppresses both Arc and c-Fos expression in fear ensemble neurons. Next, we asked whether this suppressive effect of extinction could be observed when a different IEG is used to assess neuronal activation. In a separate set of sections from the same mice, we performed immunohistochemistry against YFP and the IEG c-Fos and quantified expression in the DG. Again, there were no significant differences in overall YFP or c-Fos expression between the No Ext and Ext groups in either the dorsal or ventral DG (Fig. 1H, I), although both YFP [$F(1, 8) = 302.19$, $p < 0.0001$, $\eta_G^2 = 0.824$] and c-Fos [$F(1, 8) = 31.48$, $p = 0.0005$, $\eta_G^2 = 0.498$] were again more abundant in the dorsal DG. Reactivation (%YFP+ cells expressing c-Fos) was also once again higher in the No Ext group than the Ext group [$F(1,8) = 32.47$, $p < 0.001$, $\eta_G^2 = 0.625$] and higher overall in the ventral DG as compared to the dorsal DG [$F(1,8) = 7.801$, $p = 0.023$, $\eta_G^2 = 0.453$] (Fig. 1J). A Treatment x Region interaction [$F(1, 8) = 7.255$, $p = 0.0273$, $\eta_G^2 = 0.454$] was also detected. Pairwise comparisons of estimated marginal means confirmed that reactivation was suppressed by extinction training in the ventral DG [$t = 5.886$, $p < 0.0001$, $d = 2.96$], while the dorsal DG trended towards, but did not quite reach, significance [$t = 1.995$, $p = 0.0634$, $d = 1.41$].

We then asked whether Arc and c-Fos were expressed in the same or different populations of reactivated cells. In a separate set of sections from the same mice as above, we conducted immunohistochemistry against Arc, c-Fos, and YFP and calculated expression in the dorsal DG only (Fig. 2). Consistent with the findings above, a one-way ANOVA showed no differences between the Extinction and No Extinction groups in density of YFP+ cells [$F(1, 10) = 0.126$, $p > 0.1$, $d = 0.205$]. A two-way ANOVA against expressed IEGs (Arc+, Fos+, or Arc+/Fos+) also found no effect of treatment [$F(1, 10) = 0.131$, $p > 0.1$, $\eta_G^2 = 0.013$], though a significant effect of IEG type was detected with there being more Arc+/c-Fos+ cells than single positive Arc [$t = 15.636$, $p < 0.001$, $d = 1.48$] or c-Fos [$t = 7.943$, $p < 0.001$, $d = 0.78$] cells (Fig. 2C). This is likely due to the fact that expression of both Arc and c-Fos are triggered by neural firing and, therefore, are more likely to be expressed together. There were also more cells single positive for Arc than c-Fos [$t = 7.694$, $p < 0.001$, $d = 0.681$]. Consistent with previous findings, there was significantly more reactivation of YFP+ cells in the No Extinction group as compared to the Extinction group [$F(1,10) = 9.275$, $p = 0.012$, $\eta_G^2 = 0.263$]. A significant effect of IEG type on reactivation level [$F(2,20) = 46.576$, $p < 0.001$, $\eta_G^2 = 0.742$] and an interaction between Treatment and IEG overlap type (Arc+/YFP+, Fos+/YFP+, or Arc+/Fos+/YFP+) were also detected [$F(2, 20) = 11.49$, $p < 0.001$, $\eta_G^2 = 0.415$]. Post-hoc pairwise comparisons showed that the suppressive effect of extinction was observed in YFP+ cells co-expressing Arc and c-Fos [$t = 5.641$, $p < 0.001$, $d = 2.38$] but not in YFP+ cells expressing only Arc [$t = 0.234$, $p > 0.1$, $d = 0.153$] or c-Fos [$t = 0.214$, $p > 0.1$, $d = 0.209$; Fig. 2D]. Thus, extinction training suppresses co-expression of Arc and c-Fos in YFP-tagged fear acquisition cells.

Extinction training suppresses fear ensemble reactivation in dorsal but not ventral CA1. To determine whether the suppressive effect of extinction training on reactivation was preserved further along the hippocampal circuit, we next analyzed expression of YFP and c-Fos in the dorsal and ventral CA1 (Fig. 3A, B). A two-way ANOVA revealed a significant difference in YFP counts between the dorsal and ventral CA1 [$F(1,7) = 657.33$, $p < 0.0001$, $\eta_G^2 = 0.849$] and a significant interaction between CA1 region and treatment [$F(1,7) = 8.42$, $p = 0.023$, $\eta_G^2 = 0.163$] which did not survive post-hoc testing (all $p > 0.05$; Fig. 3C). No significant differences in c-Fos levels were detected between treatment groups or region and no interaction between variables were detected (all $p > 0.1$; Fig. 3D). Comparison of reactivation levels (YFP+/Fos+) across regions and treatments showed a significant effect of treatment [$F(1,7) = 29.194$, $p = 0.001$, $\eta_G^2 = 0.124$], region [$F(1,7) = 387.869$, $p < 0.0001$, $\eta_G^2 = 0.884$], and a significant interaction between the two [$F(1,7) = 11.479$, $p = 0.012$, $\eta_G^2 = 0.01$; Fig. 3E]. Post-hoc testing showed that while extinction training significantly decreased reactivation of the fear ensemble in the dorsal CA1 [$t = 6.086$, $p < 0.0001$, $d = 3.18$], no such suppression of reactivation was detected in the ventral CA1 [$t = 0.935$, $p = 0.366$, $d = 0.68$]. Overall, our results suggest that extinction training suppresses reactivation of fear ensembles in dorsal and ventral DG and dorsal CA1, but not ventral CA1.

snRNA-seq

Single-cell transcriptomes reveal canonical cell-types. We employed snRNA-seq analysis of the dorsal DG as an unbiased and comprehensive approach to survey the transcriptomes of cells belonging to the fear and extinction ensembles. We focused on the dorsal DG based on evidence above that the extinction-induced suppression of fear ensembles in the dorsal DG is representative of ensemble behavior across the dorsal-ventral axis of the DG and in dorsal CA1. In addition, our prior study shows that the activity of ensembles in the dorsal DG is necessary and sufficient for

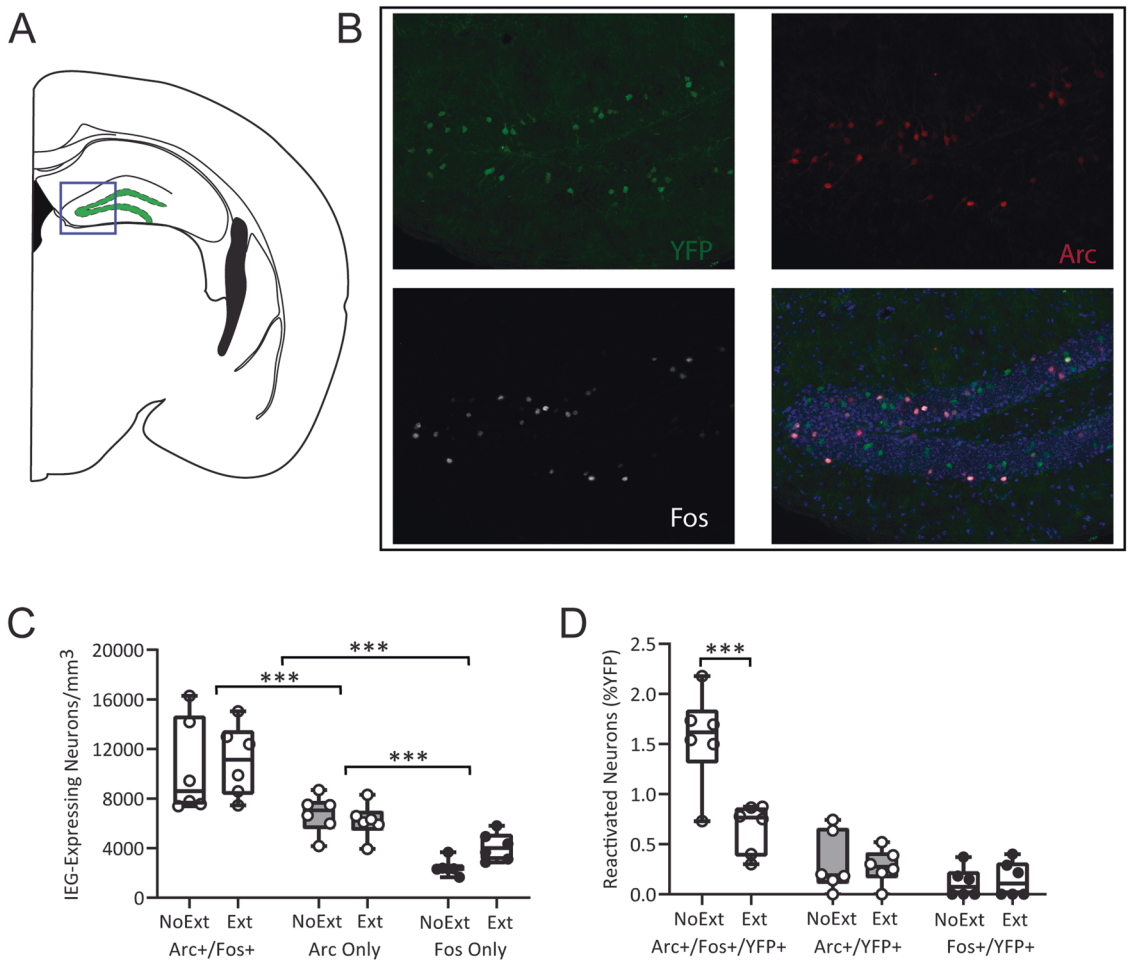

Fig. 2 Triple labeling reveals that extinction suppresses co-expression of Arc and Fos in YFP+ fear neurons in DG. A Coronal section displaying the representative location of imaging and cell counts. The blue box identifies where representative images (in **B**) were taken. **B**. Representative micrographs of YFP+, Arc+, and Fos+ immunofluorescence in tissue processed for all three antigens. **C** There was no significant difference between groups in the density of cells expressing Arc+ alone, Fos+ alone, or co-expressing Arc+/Fos+. However, the overall density of cells co-expressing Arc+ and Fos+ was significantly higher than the density of cells expressing either IEG alone. **D** Extinction training suppressed co-expression of Arc and Fos in YFP+ fear neurons but not reduce the percentage of YFP+ cells expressing only Arc or only Fos. *** $p < 0.001$.

expression of fear and extinction memories [6]. We repeated the behavioral assay as described above ($n = 3$ per group) and, as before, we observed significantly less freezing in mice that received extinction training as compared to those that did not [Fig. 4A; *t* test: $t(4) = 10.45$, $p < 0.001$]. We then collected and pooled (separately for No Ext and Ext) the dorsal DG nuclei for snRNA-seq. After demultiplexing and filtering, we recovered 19301 nuclei from the two treatment groups (Ext: 10828, No Ext: 8473). To evaluate the cell type-specific response to Fear Extinction/Recall training, we integrated the snRNA-seq datasets from both treatments and then used the Seurat integrative analysis approach revealed 17 clusters that differed in transcriptomic profiles in the integrated dataset (Fig. 4E). Based on previously identified hippocampal gene markers [25], these 17 clusters represented nine cell types. As expected, the vast majority of cells were granule cells (Ext: 57.23%; No Ext: 65.22%), although the other canonical cell types (e.g., interneurons, oligodendrocytes, astrocytes, microglia, etc.) were identified as well. In concordance with the immunohistochemistry results above (Fig. 1E–J), the number of granule cells that express *c-Fos*, *Arc*, and/or *YFP* mRNA did not differ between treatment groups (Fig. 4B, C; $\chi^2 < 1$, $p > 0.25$ in all cases), nor did the number of putative extinction ensemble cells (i.e., neurons that expressed *Arc* but not *YFP* mRNA; Fig. 4D). Note that less than 2% of granule cells expressed *c-Fos*, while more than 7% of granule cells expressed *Arc* (a ca. 3.5-fold difference). This is in marked contrast to our immunohistochemistry results, where the difference was only 1.5-fold (see Fig. 1F, I). While it is speculative at this point, it is conceivable that granule cell *c-Fos* mRNAs are quickly moved out of the nucleus upon stimulation and may thus not be as readily detectable by single nucleus mRNA-seq. Interestingly, in contrast to our immunohistochemistry results, extinction training did not reduce the fraction of *YFP* mRNA+ granule cells that co-expressed *Arc* mRNA ($\chi^2 < 1$, $p > 0.25$; Fig. 4B). We also examined levels of *Arc* mRNA expression in *YFP*+ cells (Supplementary Fig. 1), which did not differ significantly between Ext and No Ext groups (*t* test: $p = 0.12$).

Cells activated by extinction training exhibit specific transcriptomic signatures. We have previously shown that extinction training not only suppresses the reactivation of fear ensemble cells but also activates a second set of cells, the putative extinction ensemble [6]. However, little is known about the molecular identity of extinction ensemble cells or how extinction suppresses fear ensemble activity. Our dataset enabled us to investigate the transcriptomic response to extinction training at single-cell resolution. We first re-clustered all granule cells and found that

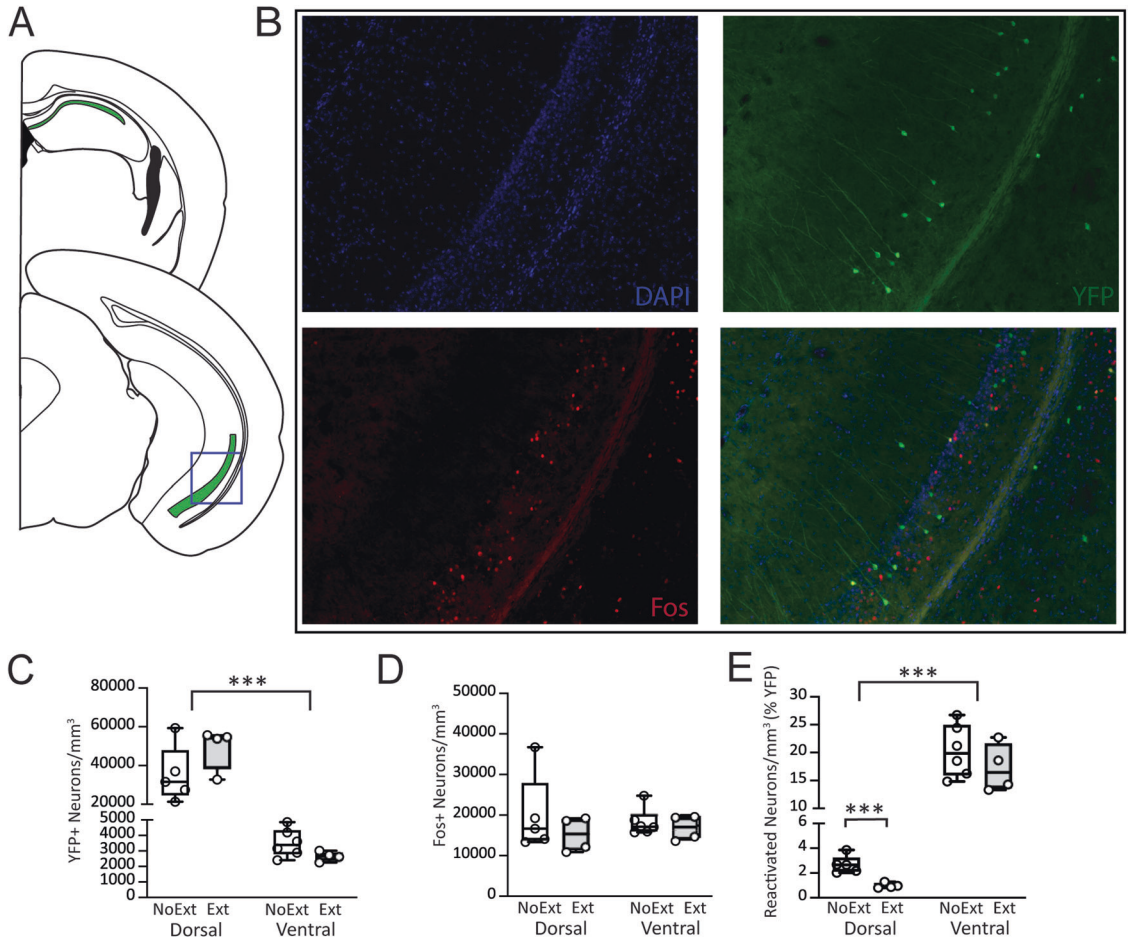

Fig. 3 Extinction suppresses reactivation of YFP+ fear neurons in dorsal but not ventral CA1. A Coronal sections displaying (in green) the area from which CA1 counts were taken. The blue box identifies where representative images (in **B**) were taken. **B** Representative images of Fos+ and YFP+ immunofluorescence in the ventral CA1. **C** There were no differences in CA1 YFP+ cell density between mice in the Ext and No Ext group. In both groups, dorsal CA1 had a higher density of YFP+ cells than ventral CA1. **D** There was no effect of extinction training or region of CA1 on Fos+ cell density. **E** In dorsal CA1, mice in the Ext group had significantly fewer fear ensemble cells reactivated (YFP+/Fos+) at final recall as compared to mice in the No Ext group. This effect was not present in the ventral CA1. In both the Ext and No Ext group, more neurons were reactivated at recall in the ventral than dorsal CA1. *** $p < 0.001$.

both No Ext and Ext groups contained a similar inventory of these cells (412 vs. 419 cells, respectively; Fig. 5A). Next, we compared the overall gene expression profiles of the two treatments for those granule cells that expressed *Arc* in the absence of *YFP* mRNA, a cell population that might contain extinction ensemble neurons. We found 1729 DEGs in these putative "extinction neurons" between Ext and No-Ext samples (Fig. 5B; Supplementary Data 1), which were significantly enriched for genes associated with neurodegenerative diseases, among other functions (Supplementary Fig. 2). Interestingly, *APOE*, a gene that encodes apolipoprotein E, was strongly overexpressed in the Ext group, consistent with previous research showing that *APOE* dysfunction impairs fear extinction [26, 27]. We next examined the transcriptome differences in YFP^{+}/Arc^{-} granule cells ($n = 399$ total) between Ext ($n = 198$) and No-Ext ($n = 201$) groups, based on the rationale that this comparison might yield additional insight into how extinction suppresses reactivation. The comparison yielded 397 DEGs ($p_{ad} < 0.05$, fc ≥ 0.2, as described in the Methods; Supplementary Data 2). As the GO analysis in Supplementary Fig. 3 shows, the affected processes are largely related to synaptic activity and synapse organizing, which are significantly increased in the No Ext condition.

We then asked whether we could identify a unique neuron subtype in the Extinction treatment that could be indicative of a fear extinction ensemble. To achieve this, we extracted putative extinction ensemble cells (*YFP-/Arc+*) from both groups (Ext: 419; No Ext: 412) and re-clustered them. Strikingly, this analysis revealed a distinct cluster (cluster 3) of the putative extinction ensemble (Fig. 5A inset): 35 of 39 (90%) of the cells in this cluster came from mice in the Ext group (FDR-adjusted $p < 0.05$ and mean $\log_2$-fold enrichment >1). Although a differential gene expression analysis was not possible due to a lack of power, given this imbalance in cell numbers, we identified the top 20 marker genes for this cluster (Supplementary Table 1). Of note, 3 of the top 5 marker genes have previously been associated with fear/anxiety- and stress-related functions in the hippocampus. Overall, 7/10 (11/20) top marker genes of this cluster have been linked to hippocampal function. None of the other clusters of extinction-activated cells differed significantly between the experimental groups. Because of the 9:1 ratio of cells between treatments in this cluster, it was unfortunately not possible to reliably identify DEGs for these putative extinction ensemble cells. However, GO analysis revealed that the cluster 3 cells were enriched for genes involved in synaptic functions (Supplementary Fig. 4).

*Secretogranin II (*scg2*) is a candidate for mediating the suppression of the contextual fear ensemble cells during extinction training.* To gain a deeper understanding of the mechanisms underlying the

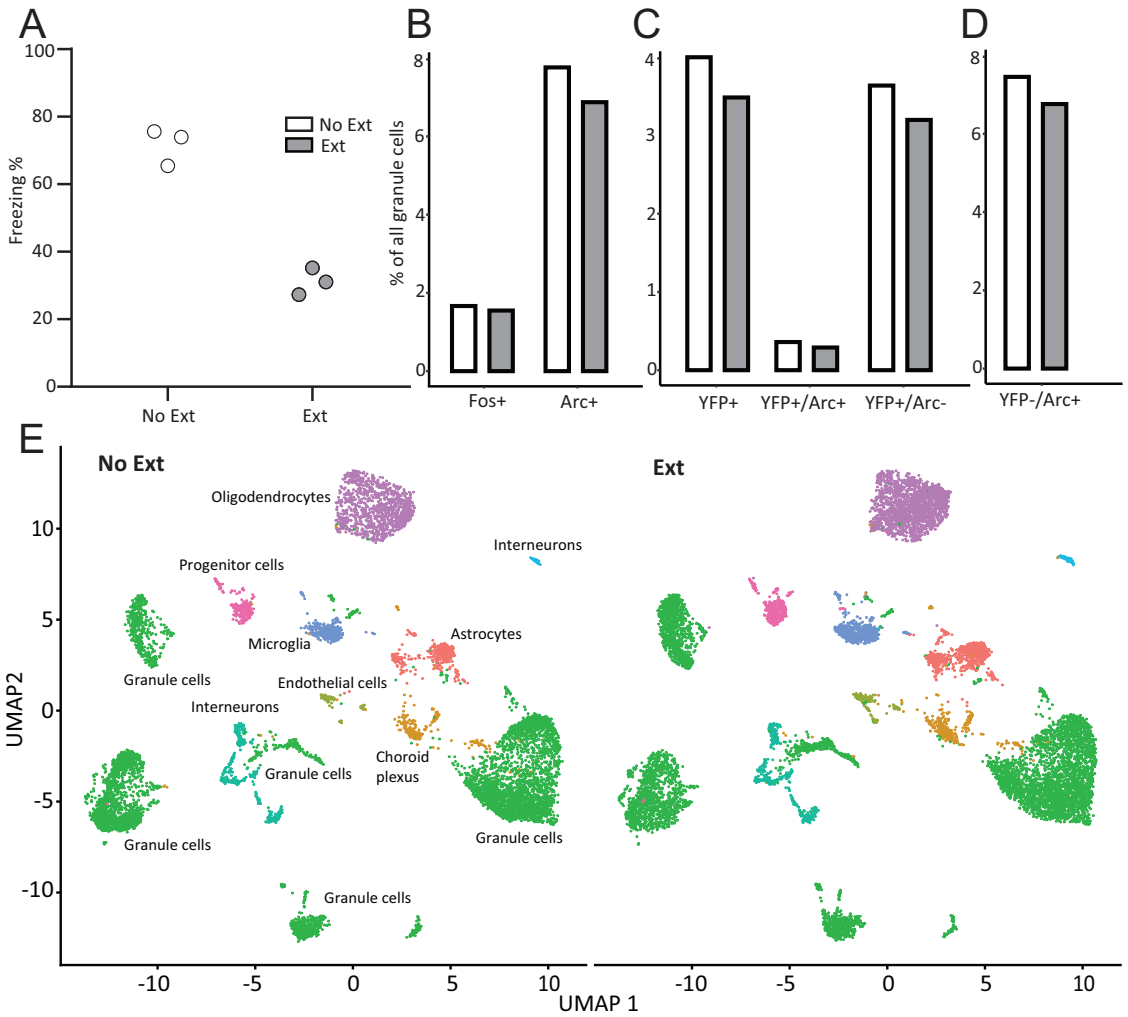

Fig. 4 snRNA-seq characterization of dorsal DG in mice after fear recall or fear extinction training. A Extinction training suppressed freezing behavior in the final test session (Ext: $n = 3$, No Ext: $n = 3$). The fraction (%) of granule cells expressing the mRNA for immediate-early genes *c-Fos* or *Arc* (**B**); *YFP* only (i.e., fear ensemble cells) or *YFP* and *Arc* (reactivated fear ensemble cells; (**C**)); and *Arc* in the absence of *YFP* (i.e., putative extinction ensemble cells; (**D**)). **E** UMAP plots for snRNA-seq data from No Ext and Ext treatments with annotated cell types.

suppression of fear ensemble cells by extinction training, it is critical to examine the transcriptional heterogeneity associated with extinction training. Possibly due to the mRNA expression kinetics of *c-Fos* [28], only a small number of granule cells expressed this IEG in our snRNA-seq dataset, and even fewer co-expressed *YFP* and *c-Fos*. However, we found that 38 granule cells co-expressed *YFP* and *Arc* (Ext: 18; No Ext: 20) in our dataset and identified 369 DEGs in these putative "reactivated fear neurons," including known targets of *c-Fos* (Fig. 5D; Supplementary Data 3). One such target is *Scg2* [29], which encodes the protein secretogranin II and its peptide metabolites. *Scg2* was highly overexpressed in these putative reactivated fear ensemble cells after fear extinction learning. Although the number of these reactivated fear neurons was small, 12 of 18 (66.7%) of these cells expressed *Scg2* in the Ext animals, while only 25% (5 of 20) of these cells did in the No Ext treatment ($\chi^2 = 6.653$, $p = 0.0099$).

Because this result was close to the statistical detection threshold of our dataset (see Methods), we repeated this analysis in the much larger population of *YFP*-expressing fear ensemble cells from both treatments (Ext: 216; No Ext: 221) and identified 1418 DEGs (Fig. 5C; Supplementary Data 4), among them *Scg2* and *Apoe*. These DEGs were enriched for pathways involved in synaptic organization and plasticity as well as genes involved in neural activity (Supplementary Fig. 5), consistent with the proposed role of *Scg2* in reorganizing inhibitory synaptic inputs in the hippocampus [29]. Finally, to better understand the treatment-specific impact of *Scg2* on the fear ensemble cells, we compared the gene expression profiles of all *Scg2* expressing fear ensemble cells between the two treatment groups (Ext: $n = 108$; No Ext: $n = 55$) and identified 803 DEGs (Supplementary Data 5). In line with the strong co-expression of *Scg2* and *Apoe* in fear acquisition neurons observed above, genes that were significantly over-expressed in the Ext treatment group were enriched for neurodegenerative disease genes, among other functions (Supplementary Fig. 6).

DISCUSSION

In the present study, we first examined activity-dependent cell tagging in ArcCreERT2::eYFP transgenic mice to indelibly label cells activated following CFC to test how extinction training affects the reactivation of fear ensemble cells. Our past research has shown that extinction suppresses fear ensemble reactivation in the DG as a whole [6], and here we first expanded on this finding by examining whether the suppressive effect of extinction extends across the dorsoventral axis of the DG. It has long been theorized that the dorsal and ventral hippocampus serve functionally distinct roles for learning and memory [30, 31]. Dorsal

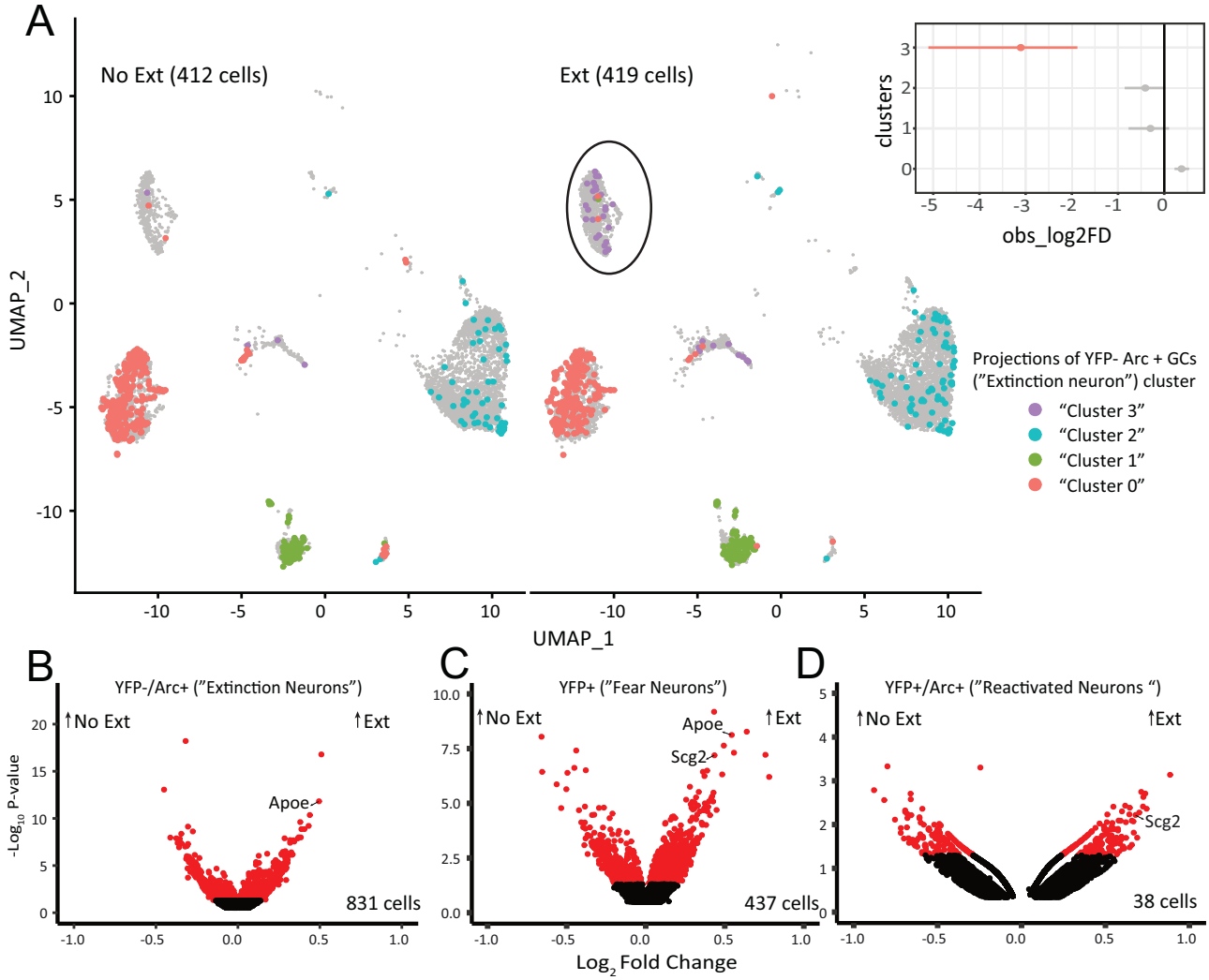

Fig. 5 Single nuclei transcription analysis of dorsal dentate gyrus granule cells. A UMAP plots show clustering of granule cells for No Ext and Ext treatments. The putative extinction ensemble cells (i.e., cells that express *Arc* in the absence of *YFP*) are indicated by color according to their cluster identity. Note that "cluster 3" cells (indicated by a circle) are almost exclusively derived from the Ext treatment. Inset shows the relative differences in cell proportions for each cluster between the Extinction and No Extinction groups based on $n = 10{,}000$ permutations with Cluster 3 (red) being the only cell cluster with an FDR-adjusted $p < 0.05$ and mean $\log_2$-fold enrichment >1. **B** Volcano plot comparing gene expression of putative extinction ensemble cells (*YFP-/Arc+*) in both treatments. DEGs are shown in red (adjusted $p \leq 0.05$). **C** Volcano plot of *YFP* expressing neurons (i.e., fear ensemble cells). **D** Volcano plot of neurons that co-express *YFP* and *Arc* (i.e., reactivated fear ensemble cells). Specific candidate genes are indicated.

hippocampal damage is consistently more disruptive to spatial tasks [32–35]. In contrast, ventral hippocampal damage/inhibition primarily disrupts emotional processes [36–40]. The distinct input/output connectivity [41] and gene expression profiles [42] of the dorsal versus ventral hippocampus further support the idea of a dorsoventral functional dichotomy. One might expect that extinction of a contextual fear association should preserve activity in cells encoding the spatial information about the context while suppressing activity in cells encoding the emotional association. That we see suppression of the fear ensemble across the dorsoventral axis of the DG following extinction suggests that both dorsal and ventral DG process information related to emotional valence. Importantly, this suppressive effect was observed with both Arc and c-Fos IEGs, lending credence to the idea that the observed changes are robust and functionally significant. It is also worth noting that while the effect of extinction on reactivation was present in both the dorsal and ventral DG, the scale of the effect was larger in the ventral DG. This may suggest a more flexible representation of valence exists within the ventral DG.

Next, we examined whether the suppressive effect of extinction on fear ensemble reactivation would persist downstream of the DG, in the CA1. In contrast to the DG, dorsal and ventral CA1 responded differently to extinction, with fear ensembles suppressed by extinction in dorsal CA1 but not ventral CA1. The lack of effect in ventral CA1 is surprising in light of the abundant evidence linking ventral CA1 to emotional processing [43–46]. The lack of extinction-mediated suppression in ventral CA1 may suggest that this region generates a valence-free context representation. Alternatively, ventral CA1 might generate a contextual fear representation that is more durable than those established elsewhere in the hippocampus, such that the ventral CA1 representation persists through extinction. Further experimentation will be needed to evaluate these ideas.

In our second experiment, we used a combination of activity-dependent cell tagging in ArcCreERT2::eYFP transgenic mice and

snRNA-seq to compare the transcriptomes of DG granule cells. We further stratified our analysis based on whether cells had been activated by fear conditioning, extinction/fear recall, or both. Unlike our findings at the protein level, we did not observe an extinction-induced suppression of *Arc* mRNA in fear neurons identified by *YFP* mRNA expression. Although *Arc* mRNA and protein were previously shown to exhibit correlated expression after novel environment exposure [47], our results raise the intriguing possibility that *Arc* mRNA and protein become decoupled after extinction training, perhaps through regulation of translational mechanisms.

In the snRNA-seq study, we discovered almost as many YFP^-/Arc^+ cells in the No Ext treatment as in the Ext treatment (412 vs. 419). One might therefore ask which, if any, of these cells are part of an emerging extinction ensemble. We speculate that the cells that constituted the small cluster of YFP^-/Arc^+ expressing granule cells that was almost exclusively limited to the Ext treatment ("cluster 3") may represent the stabilized extinction ensemble present in the Ext group after 10 sessions of extinction training. The remaining YFP^-/Arc^+ cells present in both treatment groups could be in the process of being recruited into a newly forming extinction ensemble (given that the retrieval test is also an extinction trial). Alternatively, these cells could represent different information in the two treatment groups. Characterizing these cells in detail will require larger sample sizes.

Our analysis of mRNA expression in the wider population of DG granule cells active at the fear learning time point (*YFP*+) showed that in mice that had undergone extinction training, genes related to synaptic reorganization were upregulated in the fear ensemble. One such extinction upregulated gene is *Scg2*, which encodes the protein secretogranin II (Scg2). *Scg2* was of particular interested due to recent work by Yap et al. [29], in which they demonstrate a *Scg2*-dependent mechanism for reorganizing interneuronal inhibitory inputs to hippocampal cells activated by environmental stimuli. In this work, Yap and colleagues found that CA1 principal cells activated after exposure to a novel environment subsequently displayed higher sensitivity to inhibition from neighboring parvalbumin-expressing interneurons and lower sensitivity to inhibition from cholecystokinin-expressing interneurons. This effect was dependent on *Scg2* expression within the affected CA1 principal neurons, demonstrating a role for *Scg2* in modulating the strength of inhibitory connections onto hippocampal neurons in an experience-dependent manner. The observed increase in *Scg2* expression in the fear ensemble of extinguished mice suggests that *Scg2* may play a similar role in strengthening inhibitory inputs to the fear ensemble following extinction. Notably, we also observed overexpression of the *Scg2* gene in the sparse number of DG fear ensemble cells that were reactivated in the Ext group. This suggests that *Scg2*-mediated inhibitory strengthening remains ongoing throughout the extinction process even in extinction-resistant fear ensemble cells. Finally, targeted comparison of Scg2-expressing granule cells between treatment groups revealed that in the Ext treatment, Alzheimer's disease genes showed increased expression. This finding may suggest shared mechanisms between Scg2-mediated fear extinction and neurodegenerative diseases. In line with this idea, a number of studies have demonstrated impaired fear extinction in both humans with [48] and rodent models of Alzheimer's disease [49–51].

Another notable mRNA that was upregulated in our extinction group was *APOE*. We observed *APOE* upregulation in both the fear ensemble (*YFP*+ cells) and the extinction ensemble (*YFP-, Arc*+ cells) of extinction-trained mice. *APOE* is translated into apolipoprotein E (ApoE), a lipoprotein which—along with ApoJ – is one of the primary mediators of cholesterol transport in the central nervous system [52–54]. There is intriguing prior evidence linking *APOE* to fear extinction learning. For example, mice that received targeted replacement of the endogenous mouse *APOE* gene sequence for the altered human sequence encoding for the *APOE2* isoform allele – but not the *APOE4* or *APOE3* isoforms – fail to show extinction after fear conditioning [26, 27]. Additionally, military veterans who are carriers of the *APOE2* isoform are significantly more susceptible to PTSD compared to those who produce other *APOE* isoforms [27, 55, 56]. The biological mechanisms underlying this impairment in extinction learning in individuals with the *APOE2* genotype remain unknown, but might relate to the unusually low binding affinity of *APOE2* to low-density lipoprotein receptors [57, 58]. Low-density lipoprotein receptor knockout mice display learning and memory impairments on a variety of spatial tasks [59–61] and decreased neurogenesis and synaptic bouton density within the hippocampus [62]. The failure of ApoE2 to properly bind to and activate these receptors may result in similar deficiencies. Additional research is needed to understand the role of *APOE* and other Alzheimer's risk genes in normative hippocampal learning and memory processes.

At this point we do not know whether the gene expression patterns we observed were induced by extinction or other behavioral manipulations, or whether they reflect pre-existing differences among distinct cell types or subtypes. Although DG granule cells are typically thought to comprise a single-cell type, single-cell expression studies have revealed unexpected functional heterogeneity among granule cells [63]. Similarly, in ventral CA1/subiculum, unique transcriptional signatures are associated with different input and output projections of pyramidal neurons [64, 65]. It is thus conceivable that DG fear and extinction neurons can be differentiated prior to learning based on their transcriptional profile, input/output projections, and/or other properties.

Our results should be interpreted with two important limitations in mind. One is that experimental groups exhibited different behavior, and these behavioral differences (freezing versus mobility), rather than the underlying mental states (fear versus suppression of fear) could conceivably have induced some of the transcriptional patterns we observed. A second limitation is that we cannot, in the current study, rule out spontaneous representational drift as a cause of the transcriptional and IEG expression changes we observed. Studies in the hippocampus and sensory cortex show that ensemble representations can evolve over repeated exposures to the same place or sensory stimulus [66, 67]. Such drift in hippocampal representations might explain why fear neurons were suppressed in mice that underwent extinction training. However, our previous results discount this explanation. Specifically, we found in Lacagnina et al. [6] that extinction training suppressed fear neurons, but this suppression was alleviated during spontaneous recovery 28 days after extinction. If the suppression were caused by drift, one would not expect to see fear neuron activity reemerge during spontaneous recovery. Although this suggests that extinction-induced suppression of fear neurons was not caused by representational drift, it remains possible that drift contributed to the transcriptional changes we observed.

CONCLUSION

Together, our findings demonstrate that extinction learning suppresses reactivation of neurons encoding fear associations throughout a variety of hippocampal subregions. This suppression is present across the dorsoventral axis of the hippocampus, with the possible exception of the ventral CA1 fear ensemble. The process of extinction learning also appears to preferentially activate genes that facilitate the development and formation of new synapses, suggesting that the cells recruited in the extinction ensemble actively remap their connectivity in response to extinction learning. Further investigation into the mechanisms driving the formation of an effective extinction ensemble could provide clues as to how dysfunction in the fear learning system arises and how it may be treated.

DATA AVAILABILITY

Sequence data in this publication have been deposited in the National Center for Biotechnology Single Read Archive (SRA). Other data, including behavior, cell counts, metadata, and protocols/scripts are available on the Texas Data Repository.

REFERENCES

1. Abramowitz JS, Deacon BJ, Whiteside SPH. Exposure therapy for anxiety. 2nd ed. Principles and practice. New York, NY: Guilford Press; 2019. p. 478.
2. Myers KM, Davis M. Behavioral and neural analysis of extinction. Neuron. 2002;36:567–84.
3. Rescorla RA. Spontaneous recovery. Learn Mem. 2004;11:501–9.
4. Heldt SA, Stanek L, Chhatwal JP, Ressler KJ. Hippocampus-specific deletion of BDNF in adult mice impairs spatial memory and extinction of aversive memories. Mol Psychiatry. 2007;12:656–70.
5. Bernier BE, Lacagnina AF, Ayoub A, Shue F, Zemelman BV, Krasne FB, et al. Dentate gyrus contributes to retrieval as well as encoding: evidence from context fear conditioning, recall, and extinction. J Neurosci. 2017;37:6359–71.
6. Lacagnina AF, Brockway ET, Crovetti CR, Shue F, McCarty MJ, Sattler KP, et al. Distinct hippocampal engrams control extinction and relapse of fear memory. Nat Neurosci. 2019;22:753–61.
7. Corcoran KA, Maren S. Hippocampal inactivation disrupts contextual retrieval of fear memory after extinction. J Neurosci. 2001;21:1720–6.
8. Corcoran KA, Maren S. Factors regulating the effects of hippocampal inactivation on renewal of conditional fear after extinction. Learn Mem. 2004;11:598–603.
9. Hobin JA, Ji J, Maren S. Ventral hippocampal muscimol disrupts context-specific fear memory retrieval after extinction in rats. Hippocampus. 2006;16:174–82.
10. Tayler KK, Tanaka KZ, Reijmers LG, Wiltgen BJ. Reactivation of neural ensembles during the retrieval of recent and remote memory. Curr Biol. 2013;23:99–106.
11. Denny CA, Kheirbek MA, Alba EL, Tanaka KF, Brachman RA, Laughman KB, et al. Hippocampal memory traces are differentially modulated by experience, time, and adult neurogenesis. Neuron. 2014;83:189–201.
12. Liu X, Ramirez S, Pang PT, Puryear CB, Govindarajan A, Deisseroth K, et al. Optogenetic stimulation of a hippocampal engram activates fear memory recall. Nature. 2012;484:381–5.
13. Ramirez S, Liu X, Lin PA, Suh J, Pignatelli M, Redondo RL, et al. Creating a false memory in the hippocampus. Science. 2013;341:387–91.
14. Martelotto LG. 'Frankenstein' protocol for nuclei isolation from fresh and frozen tissue for snRNAseq v2. 2019 May. Available from: https://www.protocols.io/view/frankenstein-protocol-for-nuclei-isolation-from-f-3fkgjkw.
15. Davis A, Gao R, Navin NE. SCOPIT: sample size calculations for single-cell sequencing experiments. BMC Bioinform. 2019;20:566.
16. Schmid KT, Höllbacher B, Cruceanu C, Böttcher A, Lickert H, Binder EB, et al. scPower accelerates and optimizes the design of multi-sample single cell transcriptomic studies. Nat Commun. 2021;12:6625.
17. Ewels P, Magnusson M, Lundin S, Käller M. MultiQC: summarize analysis results for multiple tools and samples in a single report. Bioinformatics. 2016;32:3047–8.
18. Wickham H, François R, Henry L, Müller K, Vaughan D. dplyr: a grammar of data manipulation. 2023. Available from: https://CRAN.R-project.org/package=dplyr.
19. Kassambara A. rstatix: pipe-friendly framework for basic statistical tests. 2023. Available from: https://CRAN.R-project.org/package=rstatix.
20. Lenth, Russel V. emmeans: estimated marginal means, aka least-squares means. 2023. Available from: https://CRAN.R-project.org/package=emmeans.
21. Olejnik S, Algina J. Generalized eta and omega squared statistics: measures of effect size for some common research designs. Psychol Methods. 2003;8:434–47.
22. Hao Y, Hao S, Andersen-Nissen E, Mauck WM, Zheng S, Butler A, et al. Integrated analysis of multimodal single-cell data. Cell. 2021;184:3573–.e29.
23. Ritchie ME, Phipson B, Wu D, Hu Y, Law CW, Shi W, et al. limma powers differential expression analyses for RNA-sequencing and microarray studies. Nucleic Acids Res. 2015;43:e47.
24. Zhou Y, Zhou B, Pache L, Chang M, Khodabakhshi AH, Tanaseichuk O, et al. Metascape provides a biologist-oriented resource for the analysis of systems-level datasets. Nat Commun. 2019;10:1523.
25. Cembrowski MS, Wang L, Sugino K, Shields BC, Spruston N. Hipposeq: a comprehensive RNA-seq database of gene expression in hippocampal principal neurons. eLife. 2016;5:e14997.
26. Olsen RHJ, Agam M, Davis MJ, Raber J. ApoE isoform-dependent deficits in extinction of contextual fear conditioning. Genes Brain Behav. 2012;11:806–12.
27. Johnson LA, Zuloaga DG, Bidiman E, Marzulla T, Weber S, Wahbeh H, et al. ApoE2 exaggerates PTSD-related behavioral, cognitive, and neuroendocrine alterations. Neuropsychopharmacology. 2015;40:2443–53.
28. Kovács KJ. Invited review c-Fos as a transcription factor: a stressful (re)view from a functional map. Neurochem Int. 1998;33:287–97.
29. Yap EL, Pettit NL, Davis CP, Nagy MA, Harmin DA, Golden E, et al. Bidirectional perisomatic inhibitory plasticity of a Fos neuronal network. Nature. 2021;590:115–21.
30. Moser MB, Moser EI. Functional differentiation in the hippocampus. Hippocampus. 1998;8:608–19.
31. Fanselow MS, Dong HW. Are the dorsal and ventral hippocampus functionally distinct structures? Neuron. 2010;1:7–19.
32. Kim JJ, Fanselow MS. Modality-specific retrograde amnesia of fear. Science. 1992;256:675–7.
33. Moser MB, Moser EI, Forrest E, Andersen P, Morris RG. Spatial learning with a minislab in the dorsal hippocampus. Proc Natl Acad Sci. 1995;92:9697–701.
34. Ferbinteanu J, McDonald RJ. Dorsal/ventral hippocampus, fornix, and conditioned place preference. Hippocampus. 2001;11:187–200.
35. Pothuizen HHJ, Zhang WN, Jongen-Relo AL, Feldon J, Yee BK. Dissociation of function between the dorsal and the ventral hippocampus in spatial learning abilities of the rat: a within-subject, within-task comparison of reference and working spatial memory. Eur J Neurosci. 2004;19:705–12.
36. Kjelstrup KG, Tuvnes FA, Steffenach HA, Murison R, Moser EI, Moser MB. Reduced fear expression after lesions of the ventral hippocampus. Proc Natl Acad Sci. 2002;99:10825–30.
37. Maren S, Holt WG. Hippocampus and pavlovian fear conditioning in rats: muscimol infusions into the ventral, but not dorsal, hippocampus impair the acquisition of conditional freezing to an auditory conditional stimulus. Behav Neurosci. 2004;118:97–110.
38. Pentkowski NS, Blanchard DC, Lever C, Litvin Y, Blanchard RJ. Effects of lesions to the dorsal and ventral hippocampus on defensive behaviors in rats. Eur J Neurosci. 2006;23:2185–96.
39. Esclassan F, Coutureau E, Di Scala G, Marchand AR. Differential contribution of dorsal and ventral hippocampus to trace and delay fear conditioning. Hippocampus. 2009;19:33–44.
40. Felix-Ortiz AC, Beyeler A, Seo C, Leppla CA, Wildes CP, Tye KM. BLA to vHPC inputs modulate anxiety-related behaviors. Neuron. 2013;79:658–64.
41. Swanson LW, Cowan WM. An autoradiographic study of the organization of the efferet connections of the hippocampal formation in the rat. J Comp Neurol. 1977;172:49–84.
42. Dong HW, Swanson LW, Chen L, Fanselow MS, Toga AW. Genomic–anatomic evidence for distinct functional domains in hippocampal field CA1. Proc Natl Acad Sci. 2009;106:11794–9.
43. Ciocchi S, Passecker J, Malagon-Vina H, Mikus N, Klausberger T. Selective information routing by ventral hippocampal CA1 projection neurons. Science. 2015;348:560–3.
44. Jimenez JC, Berry JE, Lim SC, Ong SK, Kheirbek MA, Hen R. Contextual fear memory retrieval by correlated ensembles of ventral CA1 neurons. Nat Commun. 2020;11:3492.
45. Jimenez JC, Su K, Goldberg AR, Luna VM, Biane JS, Ordek G, et al. Anxiety cells in a hippocampal-hypothalamic circuit. Neuron. 2018;97:670–.e6.
46. Parfitt GM, Nguyen R, Bang JY, Aqrabawi AJ, Tran MM, Seo DK, et al. Bidirectional control of anxiety-related behaviors in mice: role of inputs arising from the ventral hippocampus to the lateral septum and medial prefrontal cortex. Neuropsychopharmacology. 2017;42:1715–28.
47. Ramírez-Amaya V, Vazdarjanova A, Mikhael D, Rosi S, Worley PF, Barnes CA. Spatial exploration-induced arc mrna and protein expression: evidence for selective, network-specific reactivation. J Neurosci. 2005;25:1761–8.
48. Nasrouei S, Rattel JA, Liedlgruber M, Marksteiner J, Wilhelm FH. Fear acquisition and extinction deficits in amnestic mild cognitive impairment and early Alzheimer's disease. Neurobiol Aging. 2020;87:26–34.
49. Hernandez CM, Jackson NL, Hernandez AR, McMahon LL. Impairments in fear extinction memory and basolateral amygdala plasticity in the TgF344-AD rat model of Alzheimer's disease are distinct from nonpathological aging. eNeuro. 2022;9:ENEURO.0181-22.2022.
50. Bonardi C, de Pulford F, Jennings D, Pardon MC. A detailed analysis of the early context extinction deficits seen in APPswe/PS1dE9 female mice and their relevance to preclinical Alzheimer's disease. Behav Brain Res. 2011;222:89–97.
51. Rattray I, Scullion GA, Soulby A, Kendall DA, Pardon MC. The occurrence of a deficit in contextual fear extinction in adult amyloid-over-expressing TASTPM mice is independent of the strength of conditioning but can be prevented by mild novel cage stress. Behav Brain Res. 2009;200:83–90.
52. Roheim PS, Carey M, Forte T, Vega GL. Apolipoproteins in human cerebrospinal fluid. Proc Natl Acad Sci. 1979;76:4646–9.
53. Vance JE, Hayashi H. Formation and function of apolipoprotein E-containing lipoproteins in the nervous system. Biochim Biophys Acta BBA - Mol Cell Biol Lipids. 2010;1801:806–18.
54. Pitas RE, Boyles JK, Lee SH, Hui D, Weisgraber KH. Lipoproteins and their receptors in the central nervous system. Characterization of the lipoproteins in

cerebrospinal fluid and identification of apolipoprotein B,E(LDL) receptors in the brain. J Biol Chem. 1987;262:14352–60.
55. Freeman T, Roca V, Guggenheim F, Kimbrell T, Griffin WST. Neuropsychiatric associations of apolipoprotein E alleles in subjects with combat-related post-traumatic stress disorder. J Neuropsychiatry Clin Neurosci. 2005;17:541–3.
56. Kim TY, Chung HG, Shin HS, Kim SJ, Choi JH, Chung MY, et al. Apolipoprotein E gene polymorphism, alcohol use, and their interactions in combat-related post-traumatic stress disorder. Depress Anxiety. 2013;30:1194–201.
57. Weisgraber KH, Innerarity TL, Mahley RW. Abnormal lipoprotein receptor-binding activity of the human E apoprotein due to cysteine-arginine interchange at a single site. J Biol Chem. 1982;257:2518–21.
58. Wilson C, Mau T, Weisgraber KH, Wardell MR, Mahley RW, Agard DA. Salt bridge relay triggers defective LDL receptor binding by a mutant apolipoprotein. Structure. 1994;2:713–8.
59. Mulder M, Jansen PJ, Janssen BJA, van de Berg WDJ, van der Boom H, Havekes LM, et al. Low-density lipoprotein receptor-knockout mice display impaired spatial memory associated with a decreased synaptic density in the hippocampus. Neurobiol Dis. 2004;16:212–9.
60. de Oliveira J, Engel DF, de Paula GC, dos Santos DB, Lopes JB, Farina M, et al. High cholesterol diet exacerbates blood-brain barrier disruption in ldlr–/– mice: impact on cognitive function. J Alzheimers Dis. 2020;78:97–115.
61. de Oliveira J, Hort MA, Moreira ELG, Glaser V, Ribeiro-do-Valle RM, Prediger RD, et al. Positive correlation between elevated plasma cholesterol levels and cognitive impairments in LDL receptor knockout mice: relevance of cortico-cerebral mitochondrial dysfunction and oxidative stress. Neuroscience. 2011;197:99–106.
62. Mulder M, Koopmans G, Wassink G, Mansouri GA, Simard ML, Havekes LM, et al. LDL receptor deficiency results in decreased cell proliferation and presynaptic bouton density in the murine hippocampus. Neurosci Res. 2007;59:251–6.
63. Erwin SR, Sun W, Copeland M, Lindo S, Spruston N, Cembrowski MS. A sparse, spatially biased subtype of mature granule cell dominates recruitment in hippocampal-associated behaviors. Cell Rep. 2020;31:107551.
64. Cembrowski MS, Phillips MG, DiLisio SF, Shields BC, Winnubst J, Chandrashekar J, et al. Dissociable structural and functional hippocampal outputs via distinct subiculum cell classes. Cell. 2018;173:1280–.e18.
65. Gergues MM, Han KJ, Choi HS, Brown B, Clausing KJ, Turner VS, et al. Circuit and molecular architecture of a ventral hippocampal network. Nat Neurosci. 2020;23:1444–52.
66. Keinath AT, Mosser CA, Brandon MP. The representation of context in mouse hippocampus is preserved despite neural drift. Nat Commun. 2022;13:2415.
67. Delamare G, Zaki Y, Cai DJ, Clopath C. Drift of neural ensembles driven by slow fluctuations of intrinsic excitability. eLife. 2023;12:RP88053.

ACKNOWLEDGEMENTS

We thank Dr. Nihal Salem for guidance and the members of the Drew and Hofmann labs for discussion. Sequencing was performed by the Genomic Sequencing and Analysis Facility at UT Austin, Center for Biomedical Research Support (RRID# SCR_021713). Computational analyses were performed using the Biomedical Research Computing Facility at UT Austin, Center for Biomedical Research Support (RRID#: SCR_021979). This research was supported by a UT Austin Catalyst seed grant to HAH and MRD, U.S. National Institutes of Health grant R01 MH117426 to MRD, U.S. National Science Foundation grant IOS-1326187 to HAH, a U.S. Department of Justice graduate fellowship to IMC, and UT Austin Graduate School Summer Fellowships to JH and IMC, and a NIH T32 (MH106454) support to LAA.

AUTHOR CONTRIBUTIONS

AZ: experiment design; data acquisition, analysis, interpretation, visualization; drafting and revising manuscript. JH: data analysis, interpretation, visualization; drafting and revising manuscript. IMC: experiment design; data acquisition; data analysis, interpretation, visualization; drafting and revising manuscript. LAA: data analysis, interpretation, visualization; drafting and revising manuscript. HAH: experiment design; funding acquisition; data interpretation; drafting and revising manuscript; project supervision MRD: experiment design; funding acquisition; data interpretation; drafting and revising manuscript; project supervision.

COMPETING INTERESTS

The authors declare no competing interests.

ADDITIONAL INFORMATION

Supplementary information The online version contains supplementary material available at https://doi.org/10.1038/s41386-024-01897-0.

Correspondence and requests for materials should be addressed to Hans A. Hofmann or Michael R. Drew.